

Changes in Work Function of Hydrogen and Oxygen Adsorption on Pt(110) Surface Measured by Mirror Electron Microscope-LEED

C. S. Shern

Department of Physics, National Taiwan Normal University, Taipei, Taiwan 117, R.O.C.

(Received February 18, 1992; revised manuscript received May 27, 1992)

The configuration and the working principle of a mirror electron microscope-low energy electron diffraction apparatus are introduced. This apparatus is used to study the surface properties of H/Pt(110) and O/Pt(110) systems. From the changes in work function at different coverages, the results of LEED, and thermal desorption spectrum, we discussed the possible geometric structures of adsorbates.

I. INTRODUCTION

A mirror electron microscope-low energy electron diffraction (MEM-LEED) apparatus based upon an electrostatic cathode lens, which uses the sample as the mirror element, provides a powerful tool for the study of surfaces.¹⁻³ Both real space images of surface morphology (MEM mode) and diffraction images of crystal structure (LEED mode) are possible in a single instrument. Campuzans et al.⁴ used a MEM-LEED system to study the (1×2) order-disorder phase transition on a Au(110) surface. Dupuy et al.⁵ applied the MEM mode of MEM-LEED to compare the images between n-doped and p-doped regions on the Si(100) surface. Samant and Unertl⁶ used a MEM-LEED system to study the phase transition of tellurium chemisorbed on Ni(111). Shern⁷ used the same system to observe the melting behavior of small particles of lead evaporated onto a polycrystalline copper foil. Recently, Thevuthasan and Unertl⁸ used it to study the premelting behavior of a Cu(110) surface.

In addition to direct imaging of surface morphology, the MEM mode of a MEM-LEED can be used to measure the change in surface potential with high spatial resolution. In this paper, we used it to measure the changes of work function in the system of H/Pt(110) and O/Pt(110) under ultra-high-vacuum (UHV) environment.

II. PRINCIPLE OF MEM-LEED

A thin lens analog which illustrates the principles of image formation of a MEM-LEED system is shown in Fig. 1. Electron beams are emitted or reflected from the surface and pass

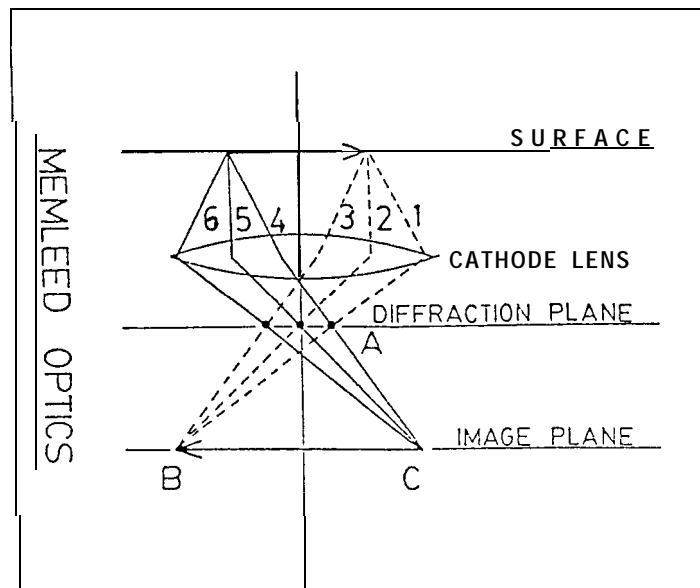


FIG. 1. Optical diagram of a MEM-LEED apparatus (after Ref. 3).

through the cathode lens. In the MEM mode, all trajectories that originate at a single point on the surface are focused at a point in the image plane. For example, trajectories 1, 2 and 3 are focused at B whereas trajectories 4, 5 and 6 are focused at C. Thus a real-space image of the surface is formed at the image plane. In the LEED mode, diffraction beams emitted parallel to the same direction but starting from different points on the surface are focused to the same point on the diffraction plane. For example, trajectories 1 and 4 intersect at point A. As in the case of light optics, the diffraction plane passes through the focal point of the lens.

Both the diffraction and real space images can thus be formed by a single optical system depending whether the image is observed in the diffraction plane or the image plane. This observation can be accomplished with a single, fixed screen if the focal length of the electrostatic lens is easily varied by changing the potentials of the lens elements. The potentials are adjusted until either the diffraction plane or image plane coincides with the observation screen.

The basic layout and dimensions of the MEM-LEED arc illustrated in Fig. 2. An energetic electron beam formed in the electron gun enters a threeelement Johansson lens.² The cathode lens consists of the anode (A), the Wehnelt (W) and the sample surface (cathode) having potentials V_A , V_W and V_C , respectively.

In the MEM mode, the high energy (8-10 KeV) electron beam is decelerated by the Wehnelt and then reflected at an equipotential surface which is at, or just outside, the sample. These slow electrons are extremely sensitive to any microfield distortions due to geometrical or electric

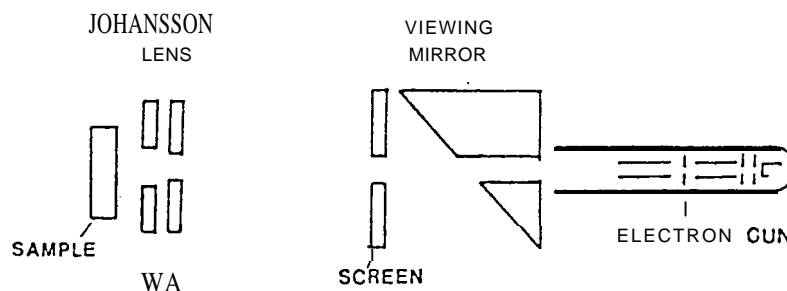


FIG. 2. (a) The schematic diagram of MEM-LEED components.

cal irregularities at the surface. For appropriate lens geometry and potentials, the reflected electrons are then reaccelerated back through the lens and form an image of the sample surface on the fluorescent viewing screen located in the image plane. The 45-degree mirror enables this image to be viewed outside the vacuum system. The magnification in the MEM mode can be adjusted, because the focal length can be varied continuously.

In the LEED mode, electrons are allowed to strike the sample at normal incidence with kinetic energy E_0 determined by the bias potential between the sample and electron gun cathode. Typical impact energies are in the range 10-100 eV. After diffraction by the crystal, the electrons are reaccelerated through the Johansson lens and the diffraction pattern is imaged on the screen located at the diffraction plane of the Johansson lens. The positions of diffraction beams in the diffraction plane are nearly independent of primary energy E_0 .⁹

The MEM mode can also be used to measure the change of the surface potential. A bias potential, V_b , is applied between the sample and the cathode of the electron gun. If V_b is smaller than the contact potential, all electrons will be reflected before they reach the sample. In this situation, no current will flow through the sample and one just see the real-space image of the surface. However, if V_b is larger than contact potential, the transmitted current I_t is not zero but increases with increasing V_b until saturation. Thus, the V_b at which I_t begins to increase abruptly is the direct measure of the change of work function. Dupuy et al.⁵ have used this method extensively.

III. EXPERIMENT

Platinum is one of the most useful material for heterogenous catalysis in the industry. For instance Pt is a catalyst for the reduction of toxic gases in automotive exhaust, such as nitrogen oxide and carbon oxide in the presence of oxygen.¹⁰ In this section, the changes of work function, $\Delta\phi$, of hydrogen and oxygen adsorbed on Pt(110) surface are studied by MEM-LEED.

Pt(110) has (1×1) bulklike structure and (1×2) reconstructed structure." The (1×1) structure is a metastable state and it will transform to a (1×2) stable reconstructed state by ther-

mal activation. This transformation is irreversible. The (1x2) reconstructed structure of fcc can be explained by a missing-row model.¹²⁻¹⁴ We studied $\Delta\phi$ in (1x2) structure of Pt(110) surface, because the (1x2) structure is the only stable phase.

The Pt(110) single crystal was purchased from ESPI corporation and was further polished in our laboratory. The sample is a disk of dimension 9.5mm in diameter and 2.0mm in thickness. 0.05 μm alumina paste was used for the final polish. The mechanically damaged layer was removed by aqua-regia solution for chemical etching. The sample orientation was checked by X-ray Laue back reflection photograph to within 0.5 degree in [110] direction. Temperature was measured with two K-type thermocouples in direct contact with opposite ends of the crystal surface. All experiments were conducted in a stainless UHV chamber. The background pressure in the UHV chamber was better than 3×10^{-10} torr.

The clean process involved several cycles of standardized Ar bombardment and annealing at 1100K. The kinetic energy of Ar ion employed for etching was 1.5 keV. The carbon contamination easily removed by introducing oxygen at a pressure of 1×10^{-7} torr for a few minutes and subsequently heating to 800K before sputtering. The sputtering and annealing cycles were repeated until a well ordered (1x2) LEED pattern was observed.

IV. RESULTS AND DISCUSSION

Hydrogen (Air Products 99.995% purity) was introduced into the UHV chamber at a pressure of 5×10^{-8} torr. Fig. 3 shows the I_t - V_b characteristic curve during hydrogen adsorption on the Pt(110)-(1x2) surface at 170K. The differences of V_b between the states of clean and covered surfaces yield the $\Delta\phi$ value. $\Delta\phi$ is positive for exposures smaller than 0.18L. The maximum positive change in work function is 0.15 eV which occurs at exposure level of 0.08L (Fig. 4a). $\Delta\phi$ become negative as exposure level are greater than 0.18L. The hydrogen coverage on the Pt(110)-(1x2) surface reaches saturation at exposure level of 20L. The maximum negative change in work function is -0.65eV which occurs at the saturated coverage (Fig. 4b).

The change of work function is caused by the presence in induced electric dipole layer between the adsorbate and the substrate. The behavior of Fig. 4 implies that hydrogen is adsorbed on the Pt(110)-(1x2) surface at different geometric positions at different coverage level. The direction of the induced dipole moment is from platinum toward hydrogen because platinum is more electronegative than hydrogen. According to the missing-row model, the Pt(110)-(1x2) surface has a roof-like structure and possesses (111) and (11 $\bar{1}$) microfacets between the valley and the row as shown in Fig. 5. This (1x2) structure formed because the interaction between the atoms is attractive for the nearest neighbors ([1 $\bar{1}$ 0] direction) whereas the interaction is repulsive for the next nearest neighbors ([001] direction). Hydrogen can be adsorbed on the row of the roof, the valley or the microfacets. Positive $\Delta\phi$ means that electrons at the Fermi level of the substrate need more energy in order to reach the vacuum level. For hydrogen

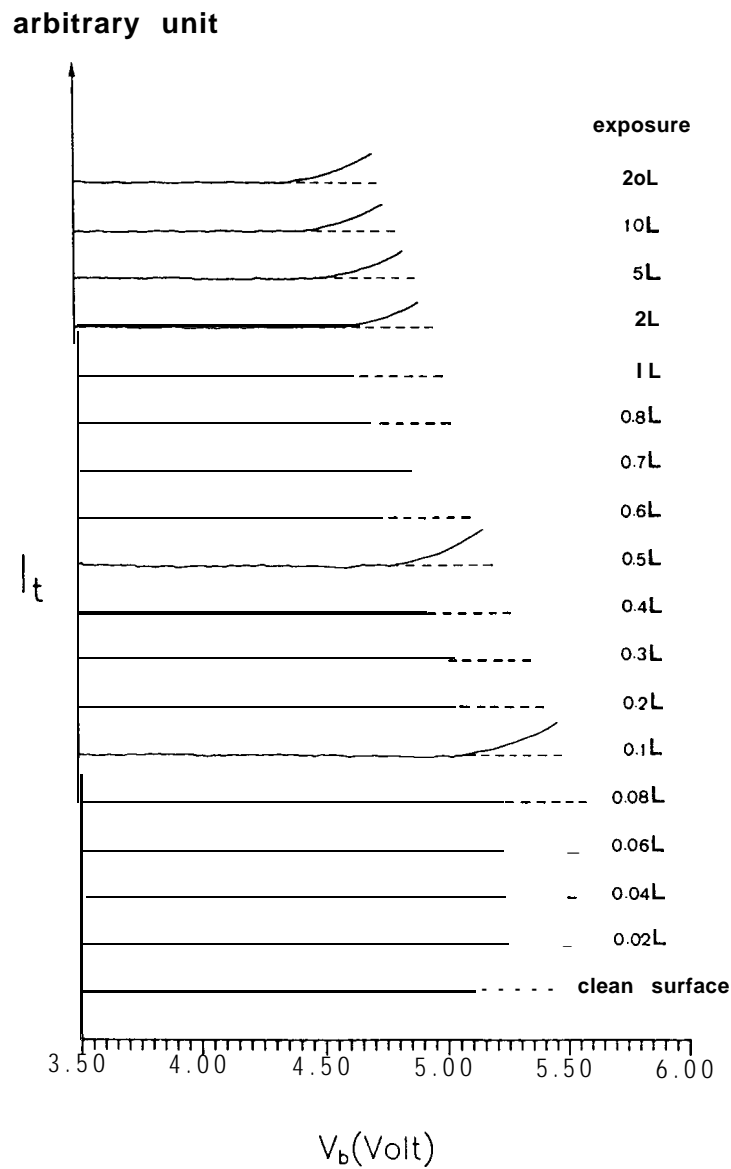
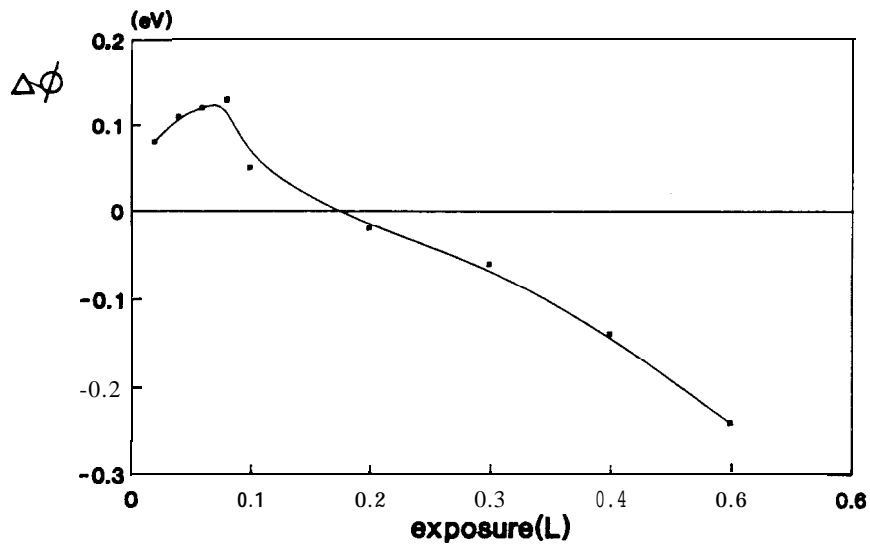
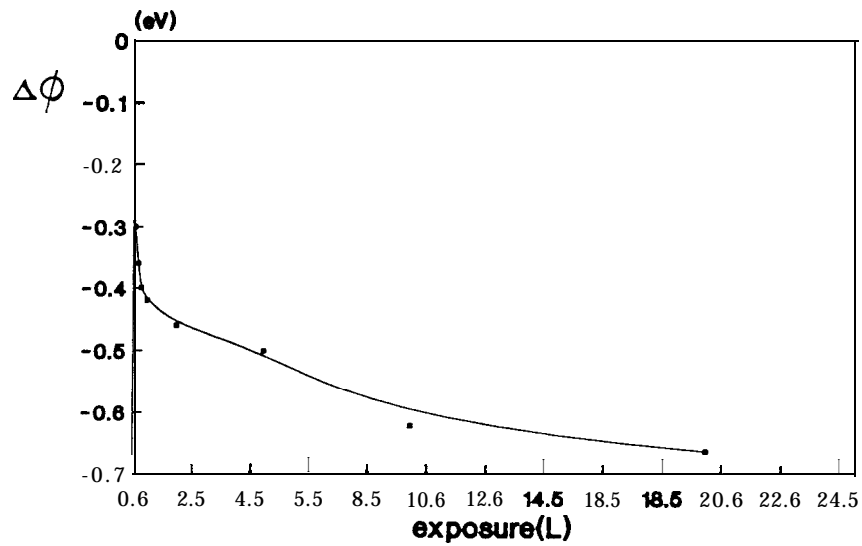


FIG. 3. I_t - V_b characteristics during hydrogen adsorption on Pt(110)-(1 X 2) surface at 170K. V_b is the bias between sample and electron gun cathode, hydrogen exposures in Langmuirs are given to the right-hand side of each curve.

adatoms lie below the image plane, the direction of the induced dipole moment will face toward the surface when they are adsorbed on the valley sites. Therefore $\Delta\phi$ will be positive. On the other hand, for hydrogen adatoms adsorbed on the rows or the (111) and (11 $\bar{1}$) microfacets $\Delta\phi$ will be negative because the direction of the induced dipole moment will be pointing outward



(a)



(b)

FIG. 4. Work function change $\Delta\phi$ extracted from data in Fig 3. (a) $\Delta\phi$ function of exposure for low hydrogen dosage. (b) $\Delta\phi$ function of exposure for higher hydrogen dosage.

the surface. The top view and side view of hydrogen atoms adsorbed on the Pt(110)-(1 \times 2) surface are shown in Fig. 6.

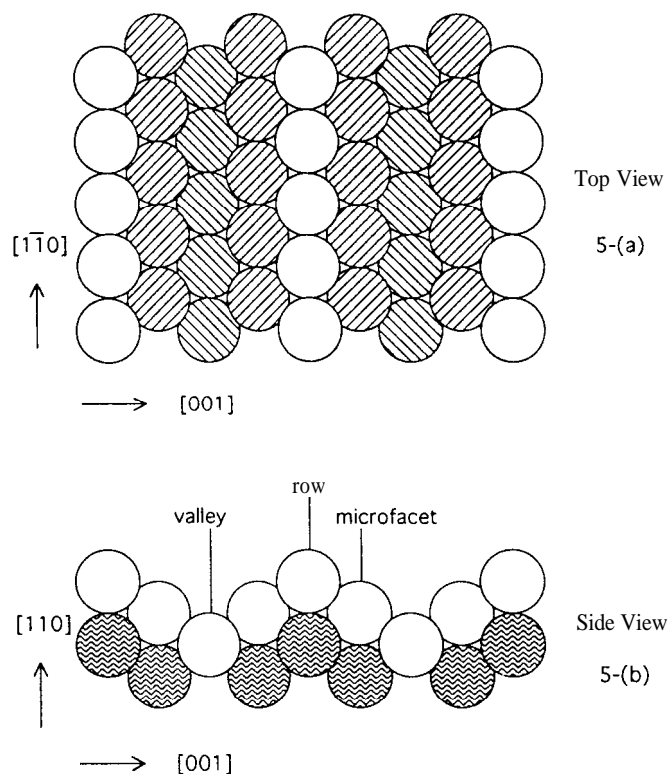


FIG. 5. Top view and side view of the reconstructed Pt(110)-(1 \times 2) surface. The atoms on the rows in $[1\bar{1}0]$ direction are missing alternatively and formed a corrugated surface.

TDS studied of Engström et al.¹⁵ and Ferrer and Bonzel¹⁶ showed that H/Pt(110)-(1 \times 2) system has two adsorption peaks, β_1 and β_2 . At lower exposure only β_2 desorption state appears. When this β_2 state is saturated, a second state β_1 is found. The peak temperature of β_2 is higher than that of β_1 . These results agree with our observation.¹⁷ Comparing these results to that of Fig. 4, it is obvious that the β_2 desorption state corresponds to $\Delta\phi > 0$ and β_1 desorption state corresponds to $\Delta\phi < 0$. Hydrogen adatoms are adsorbed on the valley sites (β_2 state) at low dosage. After the valley sites are almost filled, the adatoms begin to occupy the sites of rows and missing-row microfacets (β_1 state). Thus, hydrogen atoms adsorbed on the sites of the valleys are more stable than that of the rows and the microfacets. Therefore, the peak temperature of β_1 adsorption state is lower than that of β_2 adsorption state.

The understanding of the mechanism of oxidation reaction on metal surface is one of the important task in surface science. We have also measured $\Delta\phi$ of oxygen chemisorbed on Pt(110)-(1 \times 2) surface by the MEM-LEED.

Oxygen (Air Products, 99.99% purity) was introduced into the UHV chamber at a pressure of 2×10^{-7} torr after a clear (1 \times 2) LEED pattern was observed. The oxygen coverage on the

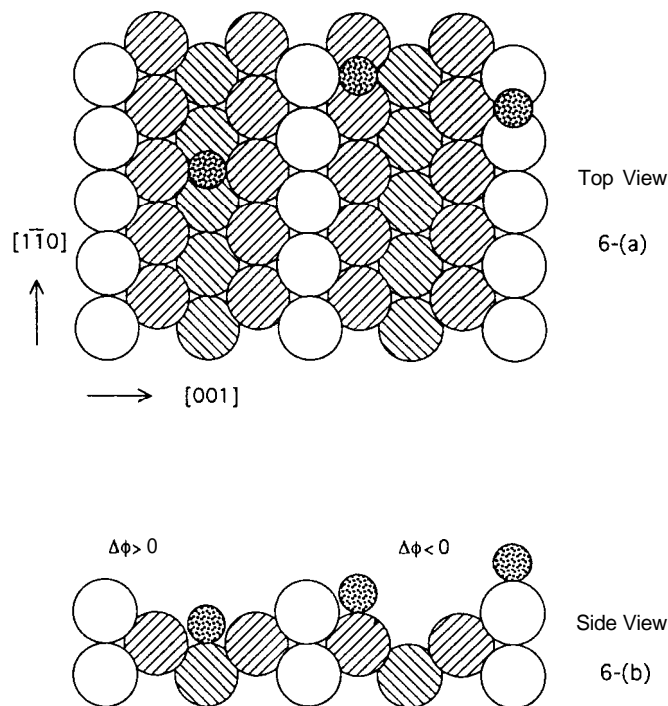


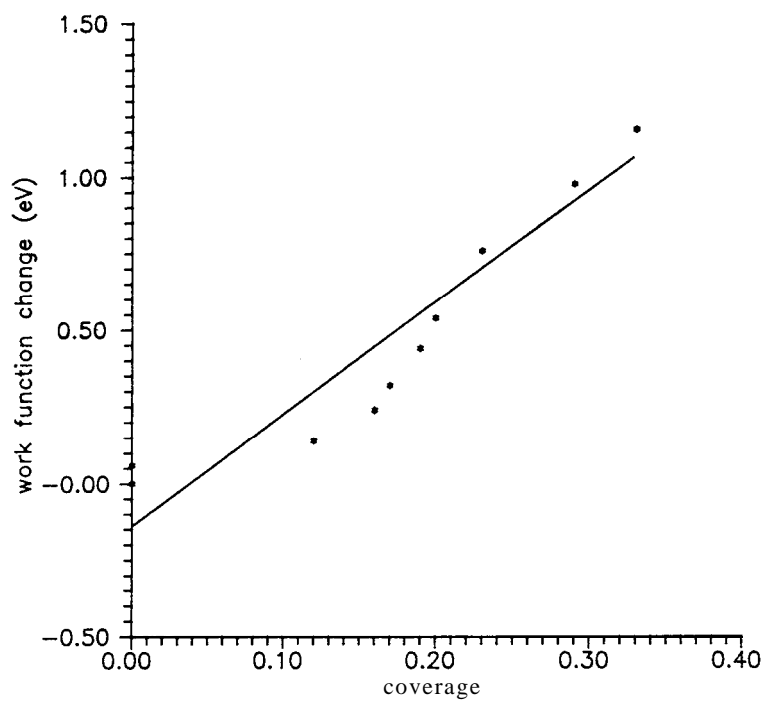
FIG. 6. Hydrogen atoms adsorbed on the valley sites ($\Delta\phi > 0$), and on the microfacet sites or on the bridge sites of the row ($\Delta\phi < 0$). Smaller circles represent H atoms, others are Pt atoms.

Pt(110) surface was measured by AES technique and calibrated according to the criteria of Ferrer and Bonzel.¹⁵ $\Delta\phi$ versus coverage, θ , of O/Pt(110) at adsorption temperature of 560K is shown in Fig. 7(a). The relation between $\Delta\phi$ and θ is linear within the experimental error. $\Delta\phi$ is always positive and the LEED pattern remains in (1x2) structure.

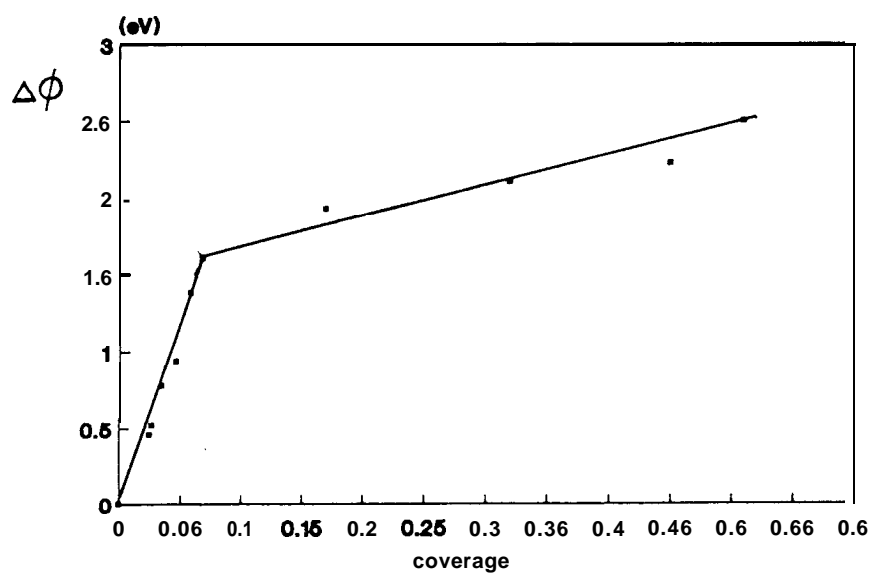
The adsorptive behavior changes abruptly when the temperature of the substrate increases to 1100K. The result is shown in Fig. 7(b). The maximum change of work function is about 2.5 eV. This large value of $\Delta\phi$ is a good evidence that PtO oxidation reaction occurs. $\Delta\phi$ has a kink at $\theta = 0.07$. This result is consistent with the LEED observation. We have observed a combined LEED pattern of C(2x2) and (1x2) at $\theta \geq 0.07$. This result implies that an expital growth of PtO belongs to the C(2x2) structure and the remaining area of the substrate is still in the (1x2) structure. The C(2x2) structure was also reported by Ducros and Merrill.¹⁸

V. CONCLUSION

A MEM-LEED apparatus has been constructed in our laboratoy. It is suitable for operating in the MEM mode and the LEED mode. In addition to the ability to observe real-space



(a)



(b)

FIG. 7. (a) $\Delta\phi$ versus coverage of O/Pt(110)-(1x2) at adsorption temperature of 560K. (b) $\Delta\phi$ versus coverage of O/Pt(110)-(1x2) at adsorption temperature of 1100K.

image, the MEM mode can also be used to measure the changes in work function. The instrument has been employed successfully to study the change in work function at 170K for hydrogen adsorbed on the Pt(110)-(1x2) surface. We observed $\Delta\phi > 0$ at low hydrogen dosage and $\Delta\phi < 0$ at high hydrogen dosage. Only $\Delta\phi > 0$ was observed for oxygen chemisorbed on the Pt(110)-(1x2) surface at $T = 560\text{K}$. An overlayer of PtO in C(2x2) structure was observed at $T = 1100\text{K}$.

ACKNOWLEDGMENTS

This work was supported by the National Science Council of ROC under grant number NSC 81-0208-M-003-17.

REFERENCES

1. M. S. Foster, J. C. Campuzano, R. F. Willis, and J. C. Dupuy, *J. Microsc.* **140**,395 (1985).
2. C. S. Shern and W. N. Unertl, *J. Vac. Sci. Technol.* **A 5**, 1266 (1987).
3. W. N. Unertl and C. S. Shern, *Mat. Res. Soc. Symp. Proc.* **208**, 261 (1991).
4. J. C. Campuzano, M. S. Foster, G. Jennings, R. F. Willis, and W. N. Unertl, *Phys. Rev. Lett.* **54**, 2648 (1984).
5. J. C. Dupuy, A. Sibai, and B. Vilotitch, *Surf. Sci.* **147**,203 (1984).
6. Samsnts and W. N. Unertl, *J. Vac. Sci. Technol.* **A 5**,**568** (1987).
7. C. S. Shern, *Chin. J. Phys.*, **26**, 1, 34 (1988).
8. S. Thevuthasan and W. N. Unertl, *Appl. Phys.* **A 51**, 1 (1990).
9. C. Berger, C. Dupuy, L. Laydevant, and R. Bernard, *J. Appl. Phys.* **48**, 5027 (1977).
10. T. Hahn and H. G. Lintz, *Surf. Sci.* **212**, 1030 (1989).
11. K. Heinz, A. Barthel, L. Hammer, and K. Muller, *Surf. Sci.* **191**, 174 (1987).
12. P. Fery, W. Moritz, and D. Wolf, *Phys. Rev.* **B38**, 7275 (1988).
13. Q. Gao and T. T. Tsong, *Phys. Rev. Lett.* **57**,452 (1986).
14. G. Anger, H. F. Berger, M. Luger, S. Feistritzer, A. Winkler, and K. D. Rendulic, *Surf. Sci. Lett.* **219**, L 583 (1989).
15. J. R. Engstrom, W. Tsai, and W. H. Weinberg, *J. Chem. Phys.* **87**, 3104 (1987).
16. S. Ferrer and H. P. Bonzel, *Surf. Sci.* **119**,234 (1982).
17. C. S. Shern, *Surf. Sci.* **264**, 171 (1992).
18. R. Ducros and R. P. Merrill, *Surf. Sci.* **55**,227 (1976).